Plasmon Absorption in grating-coupled InP HEMT and Graphene sheet for tunable THz Detection

Nima Nader Esfahani*[a,b,c], R. E. Peale[a], Christopher J. Fredricksen[a], Justin W. Cleary[b], Joshua Hendrickson[b], Walter R. Buchwald[c], Ben D. Dawson[d], and M. Ishigami[d]
[a]Department of Physics, University of Central Florida, Orlando FL, USA 32816;
[b]Air Force Research Laboratory, Sensors Directorate, Wright Patterson AFB OH 45433;
[c]Solid State Scientific Corporation, 12 Simon St. Nashua, NH 03060
[d]Department of Physics and Nanoscience Technology Center, University of Central Florida, Orlando, FL 32816

ABSTRACT

Tunable resonant absorption by plasmons in the two-dimensional electron gas (2DEG) of grating-gated InP- and Graphene-based HEMTs are investigated. Fourier-spectrometer-obtained transmission resonances are observed over a wide spectral band from mm wavelengths to THz frequencies. These results are found to be consistent with grating period and 2DEG sheet charge density dependent theoretical calculations. The temperature dependence of these transmission resonances as a function of temperature is also reported for both devices. Such devices have potential as a chip-scale frequency-agile THz imaging spectrometers for man-portable or space-based spectral-sensing applications.

Keywords: HEMT, Plasmon, terahertz, Graphene, 2DEG

1. INTRODUCTION

The excitation of plasmon resonances in the two dimensional electron gas (2DEG) of high electron mobility transistors (HEMTs) is a well-known phenomenon [1, 2]. Because the frequency of the plasmon resonance is dependent on the 2DEG sheet charge concentration, external voltages, typically used to control the sheet charge density, can also be used to control the frequency of the allowed plasmon mode [3, 4]. Due to the momentum mismatch that exists between free space optical fields and plasmon modes, the gate of the HEMT is typically fabricated into a grating and serves the dual purpose of the voltage control element for sheet charge density modulation as well as a momentum matching element for plasmon excitation.

Plasmon generation in the 2DEG of grating-gated InP HEMTs has been studied previously [3, 5, 6, 7]. In those works, discrepancies between theory and experiment in regards to the resonant absorption frequency were attributed to the incomplete transfer of charge carriers from the doped semiconductor layers to the 2DEG [8, 9]. In this paper we present terahertz transmission spectra for the gate region of an InP HEMT at room and low temperature. The HEMT layer structure differs from that of the previous studies in a way that should avoid the earlier discrepancies. A gate-grating period a = 0.5 μm was chosen so that the fundamental plasmon resonance absorption line would appear near 100 cm^{-1}.

Additionally, similar studies of Graphene-based HEMTs are reported here. Potential advantages of Graphene HEMTs are sharper resonance lines, higher THz resonance frequencies, and a broader tuning range than can be achieved using semiconductor-based 2DEGs. We previously reported CVD-grown Graphene with cm dimensions together with initial far-IR transmission measurements and theoretical predictions for plasmon resonance lineshapes and tuning [7]. Plasmon-light coupling in different Graphene structures were studied before [7, 10]. Graphene ribbon arrays showed strong coupling effects even at room temperature with absorption lines as strong as 13% [10]. In contrast to conventional 2DEGs in HEMTs, for which plasmon frequencies go as the square root of the sheet charge density n_s, it was found that for Graphene-based devices the frequencies vary as the fourth root of n_s [7, 10]. In this paper we present new transmission spectra of a grating-gated Graphene-based HEMT.

2. THEORETICAL CONSIDERATIONS

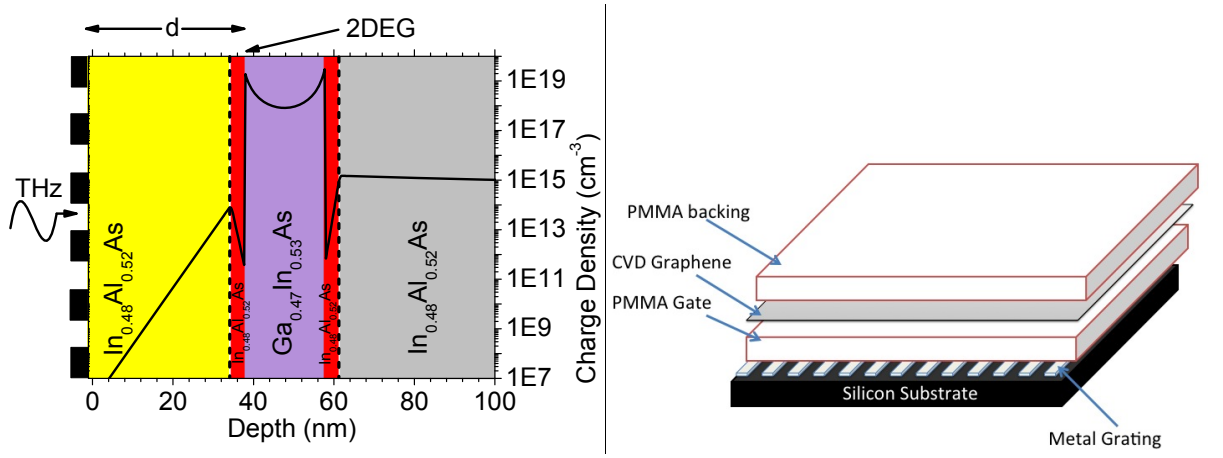

Fig. 1. (left) Schematic of grating gated InP HEMT. The different epitaxially-grown materials are indicated. Terahertz radiation is incident on the grating gate from the left. The curve indicates the calculated charge density as a function of position. The 2DEG is located a distance d from the gate. (right) Schematic of Graphene device.

The device structure is presented schematically in Fig. 1(left) for a commercial InP HEMT wafer designated PLS023B-1. The grating period a was chosen by design to be 0.5 μm with metallization ratio t/a = 0.3, where t is the width of the opening between grating bars.

Transmission spectra were calculated following the approach discussed in [2, 3, 4, 5]. Device parameters used as input were sheet charge density and relaxation time, which were determined from measured temperature dependent current-voltage (I-V)-curves. Figure 2 (left) presents calculated room-temperature spectra for different gate bias. Figure 2 (right) presents the same for 4 K sample temperature. At 300 K, the plasmon fundamental appears at 97 cm^{-1} at zero bias and red-shifts to 82 cm^{-1} under -0.2 V bias. At zero bias, a harmonic appears at 158 cm^{-1}. For low temperatures, the fundamental appears at 92 cm^{-1} for zero gate bias and red-shifts to 78 cm^{-1} for -0.2 V bias. The zero bias harmonic appears near 152 cm^{-1}.

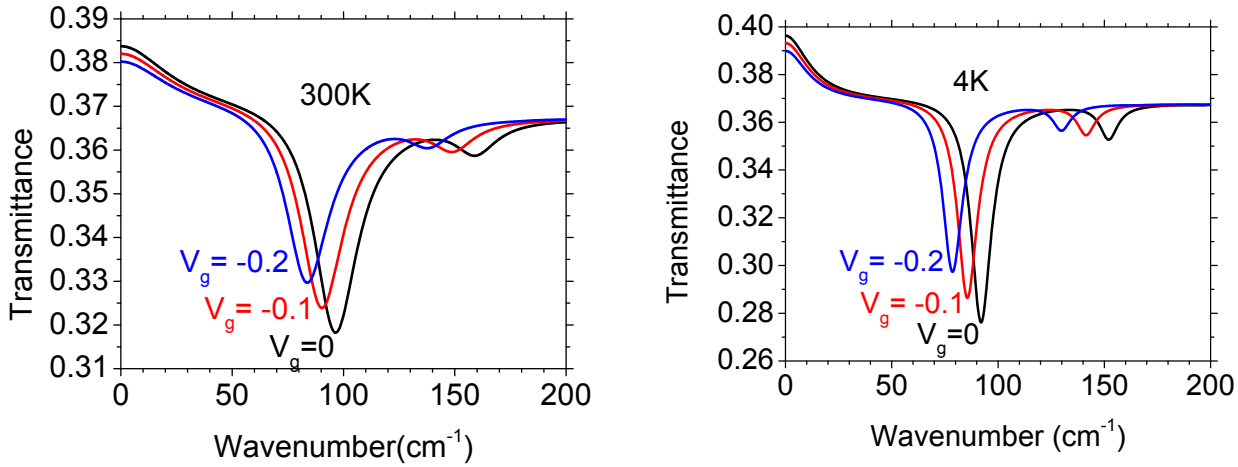

Fig. 2. Calculated Plasmon spectra of PLS023B-1 HEMT device at room (left) and helium (right) temperature for three different gate bias as labeled inside the graph.

Fig. 1 (right) presents a schematic of the Graphene-based device. This first device lacks source and drain contacts, and so is not a complete and functioning HEMT. Calculation of the expected plasmon resonance spectrum for this Graphene device requires a modification of the theory, since the carrier effective mass in this material is supposed to be zero. From the semiclassical approach of [7] based on Drude model for the 2D plasmon dispersion relation of HEMT devices,

the non-retarded dispersion for plasmons in Graphene separated by *d* from a perfectly conducting gate can be written as

$$\omega_n{}^2 = \frac{e^2 E_F q_n}{\pi\hbar^2\epsilon_0}\left(\varepsilon + \varepsilon coth(q_n d)\right)^{-1} \quad (1)$$

Where $q_n=(2\pi/a)n$, with gate grating period a = 3.4 μm, integer n, and ε = 3.3 (PMMA permitivity). The Graphene mobility is taken to be 5000 cm^2/Vs at room temperature. The calculated transmittance spectrum is presented in Figure 3, where the reference spectrum was calculated by setting sheet charge density, n_s, equal to zero. The downward sloping baseline toward long wavelength is therefore due to free carrier absorption.

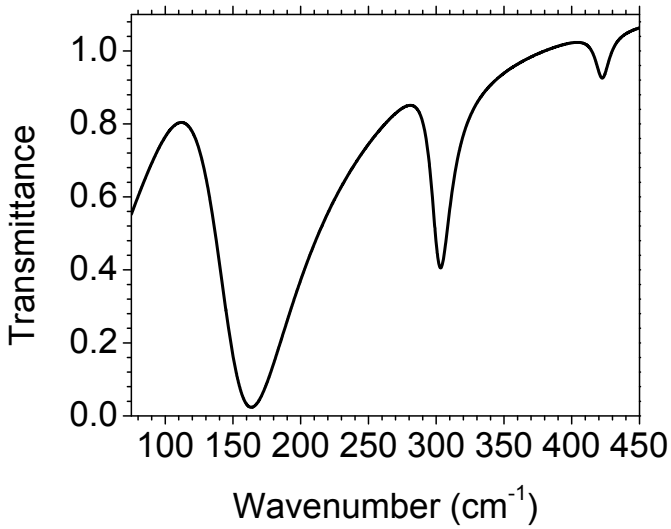

Fig. 3. Calculated transmittance spectrum of grating-gated Graphene device.

3. EXPERIMENTAL DETAILS

Metalization to form the HEMT structure was performed at Air Force Research Lab at Hanscom AFB by the authors before that facility was closed. The metallization of source, gate, and drain contacts followed the design described in [3] so that there can be no transmission of THz light except through the gate region. Fig. 4 (left) presents an optical microscope image of the device at 45x magnification. The gate grating covers the central rectangle with source and drain contacts on either side. The rest of the device is covered in overlapping deposition of gold insulated as needed by Cyclotene (BCB). The sample was then mounted on a plate having a hole aligned with the gate.

Transmission spectra through the gate region of the device were measured both at room and low temperature. Room temperature measurements were performed using a Bruker Vertex 80V Spectrometer interfaced with a Hyperion 3000 IR-microscope. The sample orientation was such that unpolarized IR radiation passed through the top grating before exiting through the substrate and being detected by a cooled Si bolometer. During these measurements, all source, gate and drain contacts were connected to ground.

Low temperature measurements were performed using a Bomem DA8 Fourier spectrometer with a Globar source, 12 and 25 micron Mylar pellicle beamsplitters and a cooled silicon (Si)-Bolometer. In this case, the sample was mounted upside down on the light cone inside the bolometer using rubber cement, similar to the experimental procedure outlined in [3]. In this configuration, pictured in Fig. 4 (right), unpolarized far-IR light first passed through the substrate of the HEMT exiting through the grating-gate before being collected by the bolometer. The plasmon-exciting local fields due to polarization of the grating bars induced by the incident THz field are still expected in this case. During these measurements, a negative gate bias was applied to the gate with the source and drain grounded in order to observe any sheet charge dependent resonant effects.

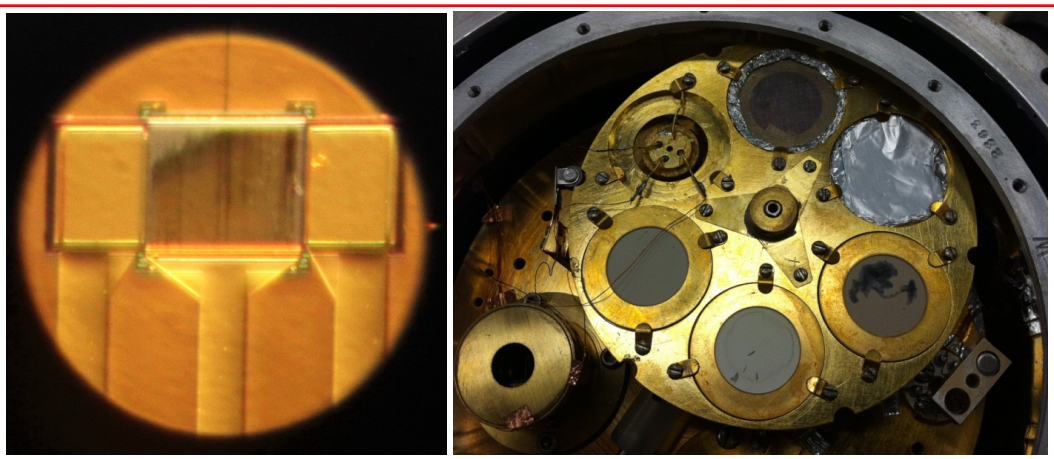

Fig. 4. (left) Optical microscope image of grating gated InP-based HEMT. The gate dimensions are 195 μm x 250μm**. (right)** A picture of the InP HEMT device mounted with grating facing the the bolometer collection cone for low-temperature measurements.

Graphene was grown on copper foil by chemical vapor deposition using a mixture of methane and hydrogen at 1000 C. To transfer Graphene, the copper/Graphene sample was first spin coated with a ~400 nm thick layer of PMMA. The foil was then placed in a solution of $FeCl_3$ so that the copper would be etched away, leaving a Graphene/PMMA stack floating on the surface. This stack is then scooped from the $FeCl_3$ and transferred to a water bath. The Graphene/PMMA stack is then scooped onto the target substrate, and baked at 70 C for about 1 hour to dry out the water. We were able to grown Graphene in areas as large as 1 cm^2 using this method. In principle any size Graphene can be grown.

A device was fabricated on a DSP silicon wafer by first depositing a gold grating (period a = 3.4 μm and openings t = 1.4 μm), and then a layer of photoresist (PMMA of thickness d = 90 nm), the Graphene (1 cm^2 cross sectional area), and PMMA stack was then deposited face down. Thus, the grating and Graphene 2DEG are separated by 90 nm. A second sample, used as reference, was identical except for the absence of Graphene. The ratio of the transmission spectra of sample and reference gives a transmittance spectrum in which any features must be due to the Graphene only. Any features due to the substrate, photoresist, or grating should divide out.

Fig. 5. (left) Photograph of the liquid nitrogen cryostat with copper-tape masking the cold-finger aperture. **(right)** Photograph of sample mounted on the cold finger of closed cycle cooler.

We measured Far-IR spectra of a Graphene-based device at 80 K using a home-built nitrogen cryostat (Fig. 5, left) and at 11 K using a closed cycle refrigerator (Fig. 5, right). The hole in the Cu 78 K coldfinger was larger than the area of the sample that was covered by Graphene, so copper tape was used to block IR from going around the sample. The sample was mounted using rubber cement. Transmittance spectra were measured using a Bomem DA8 Fourier spectrometer

with globar source, 6 micron mylar pellicle beamsplitter, and room temperature DTGS detector. The sample was oriented so that unpolarized far-IR radiation passed through the substrate and grating before passing through Graphene.

For 11 K measurements, samples were mounted on the cold finger of a helium closed cycle refrigerator using rubber cement and copper tape (Fig. 5 right). The cryostat vacuum jacket had Polyethylene windows (Fig. 6, left). The sample temperature was monitored using a silicon diode temperature sensor. Then the tailstock of the cryostat was inserted into the vacuum of the spectrometer sample compartment using an o-ring muff-coupler. (Fig. 6 right)

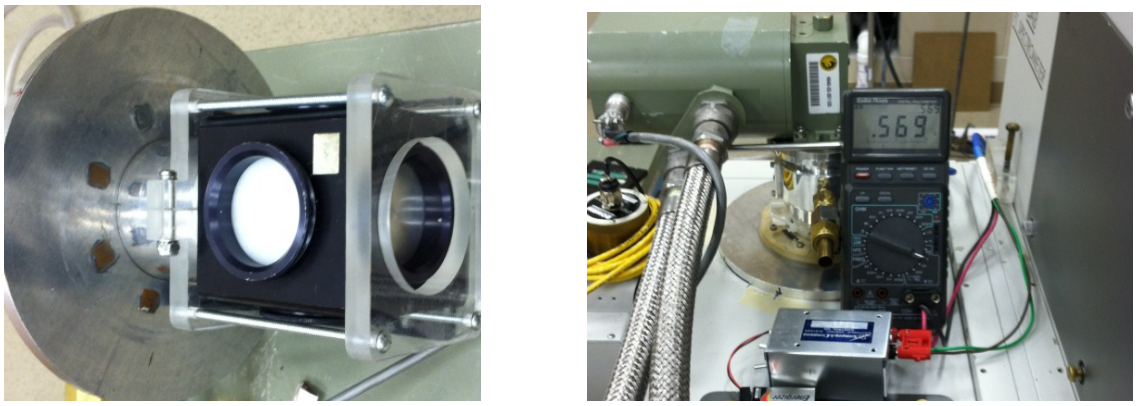

Fig. 6. (left) Photograph of the evacuated tailstock with polyethylene windows. **(right)** Photograph of the closed cycle refrigerator with tailstock inserted into evacuated spectrometer sample compartment. The DVM reads the voltage drop across a Si diode temperature sensor.

4. RESULTS

The transmission spectrum of the InP-based device at 300 K is shown in Figure 7. These measurements differ from the calculations by not having a reference devisor, so the spectrum is of raw transmitted power. Hence, the spectrum is dominated by oscillations due to the Fabry-Perot resonances inside the InP-substrate, which are not divided out. The period of these oscillations is as expected for an InP etalon of refractive index around 3.4 [11] and thickness of 154 μm. However, the amplitude of these oscillations appears strongly suppressed at 110 and 160 cm^{-1}. This is evidence of absorption lines, which spoil the Q of the etalon and lower the visibility of its fringes. These values are close to the position of the plasmon fundamental and the first overtone predicted by theory (Fig. 2), namely 97 and 158 cm^{-1} respectively. Unfortunately we didn't have the opportunity to apply gate bias to the sample and observe the tuning of the plasmon absorption lines.

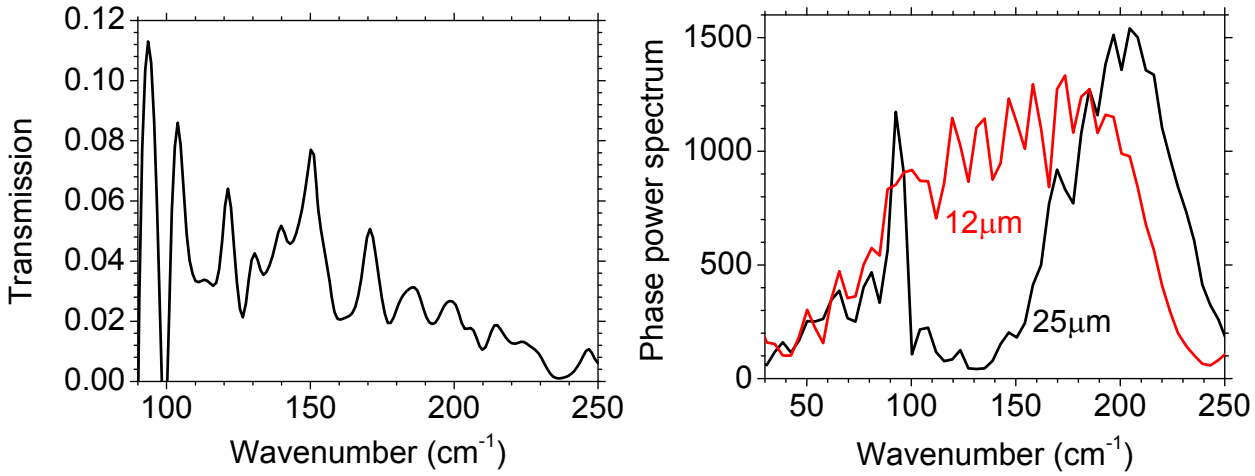

Fig. 7. (left) Grating gated InP HEMT transmission spectrum at room temperature. **(right)**Low-temperature low-resolution transmitted power spectrum for grating gated InP HEMT using two different beam splitters. Thicknesses of beam splitters are labeled beside each plot in the graph.

Low temperature transmission spectra were measured using two different beam splitters, 12 and 25 micron Mylar, to cover a wider range of frequencies. Figure 7 (right) shows the transmitted power spectra of the sample at helium temperature using the two beam splitters. The primary useful range for the 25 micron beam splitter is determined from these spectra to be 40-110 cm^{-1} with a second range of good modulation efficiency observed at 160 – 250 cm^{-1}. The useful range for the 12 micron beamsplitter is evidently 50 - 230 cm^{-1}. This beamsplitter is thus the best choice if the plasmon resonance fundamental occurs at 92 cm^{-1} as predicted by theory (Fig. 2). We note that these power spectra were collected with the sample already at helium temperature and positioned in front of the bolometer within its cryostat. Hence any plasmon features should already be present.

The spectra plotted in Fig. 7 (right) are at low resolution and were obtained from a short double sided interferogram and a complex Fast Fourier transform (FFT). This measurement is used to characterize the phase of the interferogram as a function of wavenumber. Whenever there is a low signal as in case of a strong absorption line, due to low modulation efficiency by the interferometer, the phase is poorly characterized, resulting in spectral artifacts at those wavenumber positions.

Fig. 8 (left) presents a higher resolution transmitted power spectrum using the 12 μm beamsplitter. This spectrum is obtained using a single-ended interferogram and a Cosine FFT with the phase correction obtained from the Fig. 7 (right) measurement. A strong narrow feature with derivative like line shape and ~ 2 cm^{-1} width is observed near 92 cm^{-1}. Such line shape can occur if there is an absorption line in a spectral range where the phase is poorly characterized. A strong line present during the phase characterization, even if unresolved, could cause such a phase error. While sharp features in the low resolution phase spectrum are unexpected on physical grounds, one does occur precisely at 92 cm^{-1}, as shown in Fig. 8 (right). These considerations strongly suggest the presence of a sharp strong absorption line in the sample.

There is also a suggestion of something in the higher resolution transmission spectrum (Fig. 8) at 165 cm^{-1}, and there is a corresponding feature in the low resolution phase (Fig. 8, right). Comparison with the calculated spectrum, also plotted in Fig. 8 (left), suggests that the 92 cm^{-1} feature could be identified with the plasmon fundamental and that the 165 cm^{-1} feature might be identified as the harmonic. Working against this assignment is the absence of any dependence on gate bias of the observed features, while expectations supported by calculations are for an observable red-shift with negative gate bias (Fig. 2). It was confirmed that the HEMT was working by measuring the I-V curves, which also allowed an estimate of sample temperature by comparison with earlier T-dependence characterization of device: T=10K.

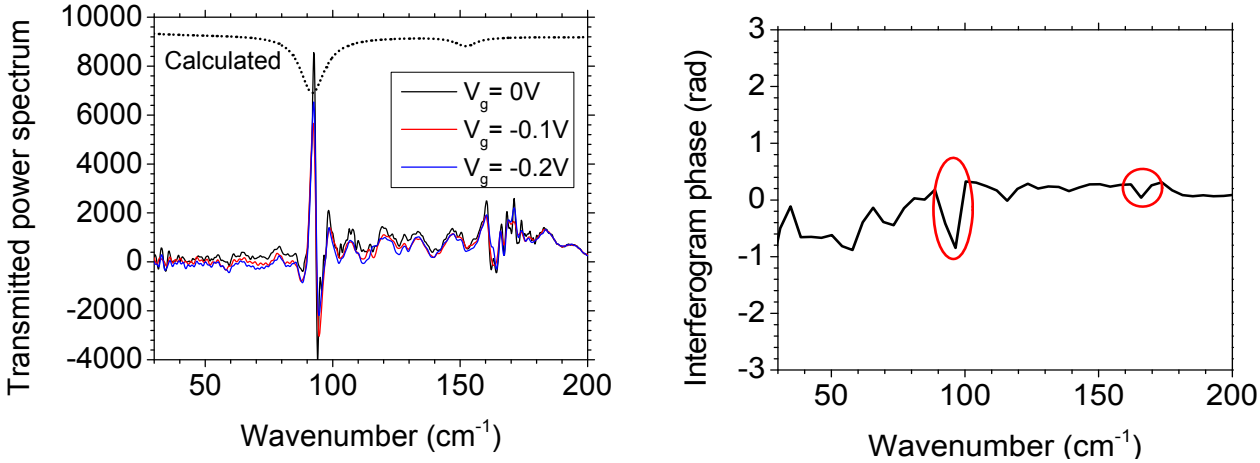

Fig. 8. (left) Transmission spectrum of InP HEMT at T = 4 K for three different gate biases. (**right**) Low resolution phase spectrum with sample in the beam. Features in the phase at wavenumbers associated with features in the transmission spectrum are circled.

The raw transmission spectra of Graphene-based device and reference samples at 80 K are presented in Fig. 9 (left). These power spectra have the same overall shape, except that the transmission is lower when Graphene is part of the structure. The useful part of the power spectrum appears to be the range of 80-360 cm^{-1}. No obvious Graphene absorption features jump out in the undivided spectrum, so if any exist, they must be weak. To reveal them, we calculated the transmittance (ratio).

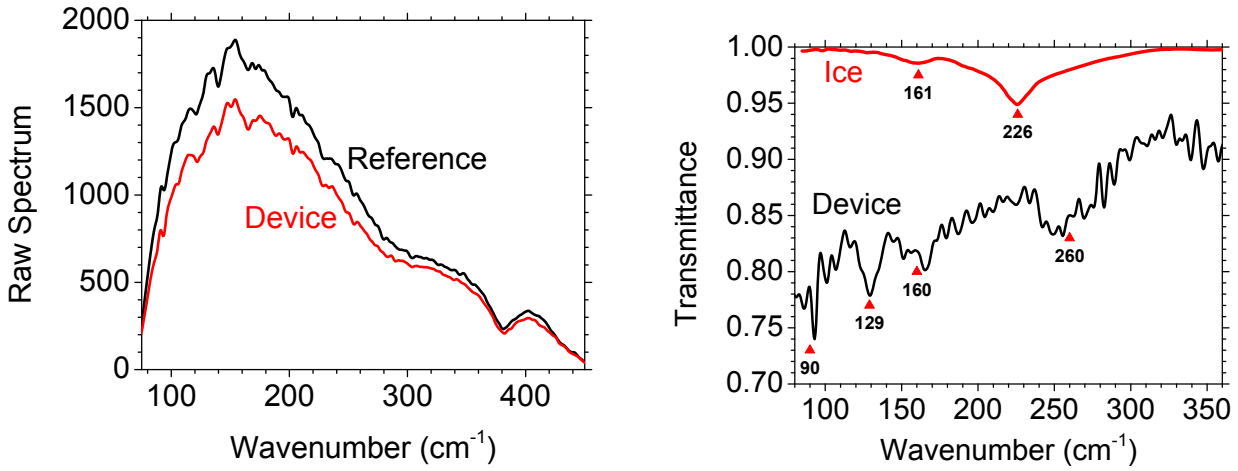

Fig. 9. (left) Raw transmission Far-IR spectra of device and reference samples. **(right)** Graphene transmittance spectrum at T=78K along with ice-band spectrum at the same frequency range as a reference for comparison. Graphs are labeled inside the plot

The transmittance spectrum (ratio of device to reference spectra) is presented in Fig. 9 (right). Four different absorption bands are observed and labeled. The ratio of the positions of the 129 and 160 cm^{-1} bands to the 90 cm^{-1} bands go roughly as the Sqrt[n], with n = 2, 3, which is as expected for the ratio of the frequencies of the nth harmonic to the fundamental (n=1) for plasmon resonances in a grating gated HEMT when d/a is greater than 0.1 [8]. When d/a is less than 0.002, the ratios go as n. In the case of our device, the d/a ratio is 0.026 which is between two limits, for this d/a, rates are expected to be 1.85 and 2.65.

There is also a broad band centered near 260 cm^{-1} which is twice the frequency of band at 129 cm^{-1}. This band can be interpreted as the fundamental in smaller d/a. However, the position of this band is does not fit well any expectations based on equation 1. Then the band centered at 250 cm^{-1} will be the second harmonics.

A thin layer of ice always forms on the sample surface during 80K spectral measurements using our home built cryostat. This occurs because the vacuum of the spectrometer sample compartment is the only insulation around 80 K coldfinger, and this vacuum is no better than 0.1 Torr. The Far-IR absorption bands of thin ice were measured separately using a polyethylene substrate at 80K. This spectrum is also presented in fig. 9 (right). The weak Ice-band at 161cm^{-1} coincides with a band in the Graphene spectrum, but the absence of the stronger 226cm^{-1} ice-band suggests an accidental coincidence.

The raw transmission power spectra of device and reference samples at 11K are presented in Figure 10 (left). The useful power spectrum covers the range 85-420 cm^{-1}. The corresponding transmittance spectrum is presented in figure 10 (right) along with the 80K spectrum for comparison.

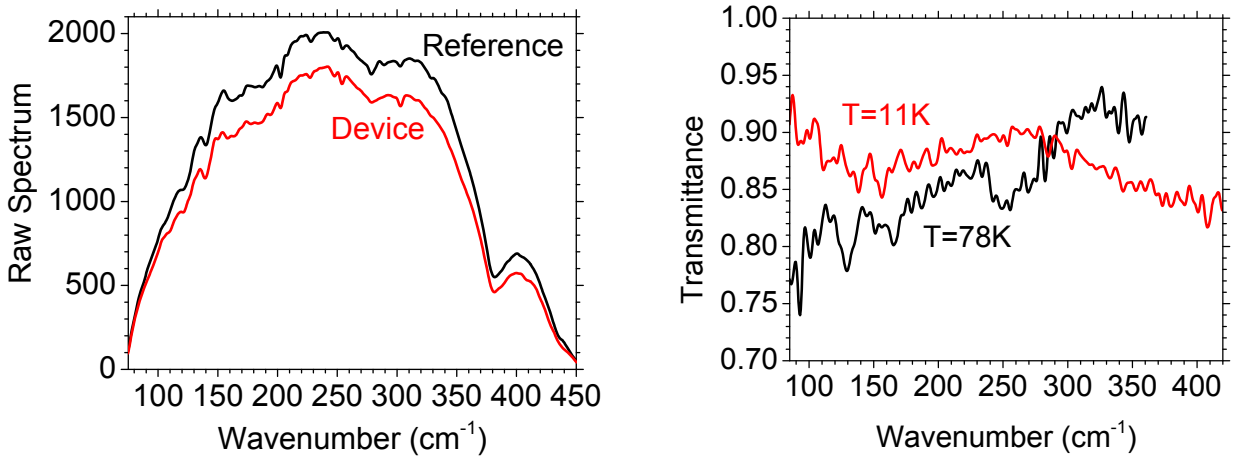

Fig. 10. (left) Raw transmission Far-IR spectra of device and reference samples. **(Right)** Graphene transmittance spectrum at T=11K along with 80K spectrum for comparison. Graphs are labeled inside the plot

5. SUMMARY

Two samples of InP- and Graphene-based HEMTs were studied to reveal the behavior of their plasmonic transmission spectrum at room and low temperatures. The InP-based HEMT device showed strong evidence of the presence of plasmon absorption lines at both room and low temperature, although they were not tuned by gate bias. The wavenumbers of the first and second harmonics were in good agreement with the ones predicted by theory presented by A. H. Macdonald [2]. Transmission spectra of Graphene-based device were measured at 80K and 4K. Different features can be observed in the spectra but they are not in complete agreement with the modified dispersion relation presented in [7]. Although in dispersion relation, plasmon frequency has the same relations with charge carrier density and grating period as of observed by [10], we are not sure if this semi-classical model can explain Graphene's plasmon-light coupling very well.

6. ACKNOWLEDGMENTS

This work was supported by AFOSR grant FA95501010030, Program Manager Gernot Pomrenke. BDD and MI acknowledge the support by the Intelligence Community Postdoctoral Fellowship Program.

REFERENCES

[1] Allen, S. J., Tsui, D. C. and Logan R. A., "Observation of the Two-Dimensional Plasmon in Silicon Inversion Layers", Phys. Rev. Lett. **38**, 980 (1977).
[2] Zheng, L., Schaich, W. L. and MacDonald, A. H., "Theory of two-dimensional grating couplers, Phys. Rev. B **41**, 8493 (1990).
[3] Saxena, H., Peale, R. E. and Buchwald, W. R., "Tunable two-dimentional Plasmon resonances in an InGaAs/InP HEMT", J. Appli. Phys. **105,** 113101 (2009).
[4] Grinberg, A. A. and Shur, M., "A new analytical model for heterostructure field-effect transistors", J. Appl. Phys. **65**, 2116 (1989).
[5] Nader Esfahani, N., Peale, R. E., Cleary, J. and Buchwald W. R., "Plasmon resonance response to millimeter-waves of grating-gated InGaAs/InP HEMT," Proc. SPIE 8023-27 (2011)

[6] Peale, R. E., Saxena, H., Buchwald, W. R., Dyer, G. C. and Allen, S. J., "Tunable THz plasmon resonances in InGaAs/InP HEMT," Proc. SPIE 7311-17 (2009)
[7] Peale, R. E., Nader Esfahani, N., Fredricksen, C. J., Medhi G., Cleary, J. W., Hendrickson, J., Buchwald, W. R., Saxena, H., Edwards, O. J., Lodge, M. S., Dawson, B. D. and Ishigami, M., "InP- and Graphene-based grating-gated transistors for tunable THz and mm-wave detection", Proc. SPIE 8164 -7 (2011).
[8] Peale, R. E., Saxena, H., Buchwald, W. R., Aizin, G., Muravjov, A. V., Veksler, B. D., Pala, N., Hu X., Gaska, R. and Shur, M. S., "Grating-gate tunable plasmon absorption in InP and GaN based HEMTs," Proc. SPIE 7467-25 (2009).
[9] Cleary, J. W., Peale, R. E., Saxena, H., and Buchwald, W. R., "Investigation of plasmonic resonances in the two-dimensional electron gas of an InGaAs/InP high electron mobility transistor," Proc. SPIE 8023, 80230X (2011)
[10] Ju, L., Geng, B., Horng, J., Girit, C., Martin, M., Hao, Z., Bechtel, H. A., Liang, X., Zettl, A., Shen, Y. R. and Wang F., "Graphene plasmonics for tunable terahertz metamaterials", Nat. Nanotechnol. 6, 630– 634 (2011)
[11] Palik, E., [Handbook of Optical Constants of Solids, Vol. I], Academic Press Inc., San Diego, London and Boston, 503-516 (1985).